Eur Biophys J (1995) 23: 413–421

European Biophysics Journal

Investigation of ion binding to the cytoplasmic binding sites of the Na,K-pump

Susann Schulz, Hans-Jürgen Apell

Department of Biology, University of Konstanz, Postfach 55 60 M635, D-78434 Konstanz, Germany
(Tel.: +49-7531-882253, Fax: +49-7531-883183, e-mail: hjapell@dg1.chemie.uni-konstanz.de)

Received: 14 September 1994 / Accepted in revised form: 24 November 1994

Abstract. A dual-wavelength fluorimeter was constructed, which used two light emitting diodes (LEDs) to excite the fluorescence dye RH 421 alternately with two different wavelengths. The ratio of the emissions at the two excitation wavelengths provided a drift-insensitive signal, which allowed detection of very small changes of the fluorescence intensity. Those small changes were induced by ion binding and release in conformation E_1 of the Na,K-ATPase. Titration experiments were performed to determine equilibrium dissociation constants (± standard deviation) for each step in the complete binding and release sequence: 0.12 ± 0.01 mM ($E_2(K_2) \leftrightarrow KE_1$), 0.08 ± 0.01 mM ($KE_1 \leftrightarrow E_1$), 3.0 ± 0.2 mM ($NaE_1 \leftrightarrow E_1$), 5.2 ± 0.4 mM ($Na_2E_1 \leftrightarrow NaE_1$) and 6.5 ± 0.4 mM ($Na_3E_1 \leftrightarrow Na_2E_1$) at pH 7.2 and T = 16 °C. These numbers show that the affinities of the binding sites exposed to the cytoplasm, are higher for K^+ than for Na^+ ions, similar to what was found on the extracellular side. The physiological requirement for extrusion of Na^+ from the cytoplasm, and for import of K^+ from the extracellular medium seems to be facilitated not by favorable binding affinities in state E_1 but by the two ATP-driven reaction steps of the cycle, $E_2(K_2) + ATP \rightarrow K_2E_1 \cdot ATP$ and $Na_3E_1 \cdot ATP \leftrightarrow (Na_3)E_1$-P, which border the ion exchange reactions at the binding sites in conformation E_1.

Key words: Na,K-ATPase – Ion binding – Equilibrium dissociation constants – Electric field sensitive fluorescence dyes – Dual wavelength fluorescence

Introduction

Ion transport by the Na,K-ATPase involves a sequence of conformational transitions and ion binding and release reactions (Glynn 1985; Jørgensen and Andersen 1988; Läuger 1991). In the course of the transport cycle the enzyme can assume two principal conformations E_1 and E_2 with inward-facing (E_1) and outward-facing (E_2) ion-binding sites. Under physiological conditions the transport process is believed to be promoted by the different relative ion affinities of the binding sites in the two conformations: in E_1 binding of sodium is preferred over potassium, and vice versa in E_2 (Simons 1974; Läuger 1991).

The transport stoichiometry of the Na,K-ATPase is well known: under physiological conditions three sodium ions are moved out of the cell and two potassium ions into the cytoplasm per cycle. Since one positive net charge per turnover is moved out of the cell, producing a contribution to the transmembrane electric current, in at least one reaction step charge is moved through the membrane (protein) dielectric, and is said to be electrogenic (Läuger 1991). Various experimental evidence has been presented that ion binding and release reactions are involved in the electrogenicity of the transport. Several of these investigations were performed by an optical method. It was shown that styryl dyes, especially RH 421, can be used to detect charge-translocating partial reactions of the Na,K-ATPase (Klodos and Forbush 1988; Stürmer et al. 1991; Forbush and Klodos 1991; Pratap et al. 1991). Although the mechanism has not yet been clarified completely, it has been demonstrated that in the flat membrane fragments containing Na,K-ATPase in high density, RH 421 acts as an indicator of the local electric fields generated by uncompensated charges inside the Na,K-ATPase (Bühler et al. 1991).

The structure of the binding sites, and the mechanisms that generate the binding affinities, are not known so far (Jørgensen 1992). Indirect evidence on their structure was collected by biochemical and biophysical investigations. Negatively charged amino acids were identified as contributing to the ion-binding moiety (Goldshleger et al. 1992; Argüello and Kaplan 1994). Electrophysiological and optical studies have provided evidence that the binding sites are buried within the protein in its E_2 conformation (Stürmer et al. 1991; Gadsby et al. 1993; Sagar and Rakowski 1994, Wuddel et al. 1994), and the the sodium-specific site in the E_1 conformation is also situated within the protein dielectric (Heyse et al. 1994). Ion binding stud-

Correspondence to: H.-J. Apell

ies with trypsin-digested protein, so called 19-kDA fragments, demonstrated that almost 50% of the protein mass that protrudes from the cytoplasmic surface of the membrane can be removed without altering the cytoplasmic ion-binding properties (Karlish et al. 1990; Capasso et al. 1992; Schwappach et al. 1994).

Many attempts were made to determine binding affinities for Na^+ and K^+ by studies with radioactive ions. However, owing to experimental constraints only apparent affinities could be given (Jensen et al. 1984; Homerada et al. 1987; Esmann 1994); apparent affinities are defined as the reciprocal of the half-saturating concentration for the observed ion binding.

The aim of this paper is the introduction of a new fluorescence detection assay, which increased the sensitivity to RH 421 signal, and its application to determine binding affinities of the Na,K-ATPase for Na^+ and K^+ ions on the sites presented to the cytoplasm in the E_1 conformation. Because the properties of RH 421 allow direct discrimination between states with different numbers of ions bound, the experiments could be restricted on the reaction sequence, which covers only the binding and release reactions,

$$Na_3E_1 \xleftarrow{K_3} Na_2E_1 \xleftarrow{K_2} NaE_1 \xleftarrow{K_1} E_1 \xleftarrow{K_4} KE_1 \xleftarrow{K_5} E_2(K_2) \quad (1)$$

by choosing buffer compositions without ATP and inorganic phosphate, P_i. Although the Na,K-ATPase is investigated in open membrane fragments, the sites can be assumed to be cytoplasmic. This is shown both by the high affinity for Na^+ and the fact that, in the presence of Mg^{2+} in the medium, the enzyme is in an E_1 form (Skou and Esmann 1980), a state in which Na^+ sites are oriented towards the cytoplasmic surface (Karlish and Pick 1981).

Materials and methods

Materials

Sodium dodecylsulfate (SDS) was obtained from Pierce Chemical (Rockford, IL, USA). Phosphoenolpyruvate, pyruvate kinase, lactate dehydrogenase, NADH and ATP (disodium salt, Sonderqualität) were from Boehringer (Mannheim, Germany). RH 421 was purchased from Molecular Probes (Eugene, OR, USA). The purity of the dye was checked by thin-layer chromatography. Ethylenediamine tetraacetic acid (EDTA) and all other reagents (at least analytical grade) were from Merck (Darmstadt, Germany).

Protein preparation

Na,K-ATPase was prepared from the outer medulla of rabbit kidneys using procedure C of Jørgensen (1974). This method yields purified enzyme in the form of membrane fragments containing about 0.8 mg phospholipid and 0.2 mg cholesterol per mg protein (Bühler et al. 1991). The specific ATPase activity was determined by the pyruvate kinase/lactate dehydrogenase assay (Schwartz et al. 1971). The protein concentration was determined by the Lowry method (Lowry et al. 1951), using bovine serum albumin as a standard. For most preparations the specific activity was in the range 2000 to 2300 μmol P_i per hr and mg protein at 37 °C. The suspension of Na,K-ATPase-rich-membrane fragments (about 3 mg protein per ml) in buffer (25 mM imidazole sulfate, pH 7.5, 1 m*M* EDTA, 10 mg/ml sucrose) was frozen in samples of 100 μl; in this form the preparation could be stored for several months at –70 °C without significant loss of activity.

Fluorescence measurements

Fluorescence spectra were determined with a Perkin-Elmer Luminometer LS 50B. The thermostated cell holder was equipped with a magnetic stirrer. In addition to spectrometric analyses, this equipment was also used to study ion binding to Na,K-ATPase-containing membrane fragments. For these experiments with RH 421, the excitation wavelength was set to 580 nm (slit width 15 nm) and the emission wavelength to 660 nm (slit width 15 nm). If not otherwise indicated, the experiments were carried out at 16 °C.

Dual wavelength experiments with RH 421-labeled membrane fragments were performed in a specially designed fluorimeter. When RH 421 experiments are carried out in a standard setup, a non specific drift of the fluorescence intensity can be observed in the range 0.2–2% per min. To correct for these effects the fluorescence was detected at two wavelengths. One wavelength produced a signal which was characteristic for the protein function, the other wavelength monitored information on the dye concentration in the illuminated volume. In contrast to the calcium indicator FURA 2, it is not possible to find an isosbestic wavelength. Changes of the electric field, which are induced by the protein function, cause (small) shifts of the whole absorption spectrum of RH 421. Therefore we selected a function-specific excitation at $\lambda = 585$ nm, which is the wavelength normally monitored with the standard equipment, and a broad band excitation (420 nm $< \lambda <$ 610 nm) as reference, which covers most of the absorption spectrum and so electric-field induced shifts do not significantly change the absorbance.

A cross section of the instrument is shown schematically in Fig. 1 A. The body is made from aluminium, is equipped with an electromagnetic stirring device underneath the buffer-containing cell, and can be thermostated. Two light emitting diodes (LEDs) are used as light sources, which are mounted at parabolic reflectors at a distance of 8 mm from the cell. To produce the reference signal a "blue" LED with an emission maximum of 475 nm was chosen. The data signal is excited by a combination of a "yellow" LED ($\lambda_{max} = 585$ nm) and a narrow-band interference filter with a maximum transmission at 585 nm and a half width of 26 nm. In Fig. 1 B the absorption spectrum of RH 421-labeled membrane fragments and the emission spectra of the LEDs are superimposed. In front of the entrance window of the photomultiplier (PM) a cut-off filter ($\lambda_{transmission} > 590$ nm) and a narrow-band interference fil-

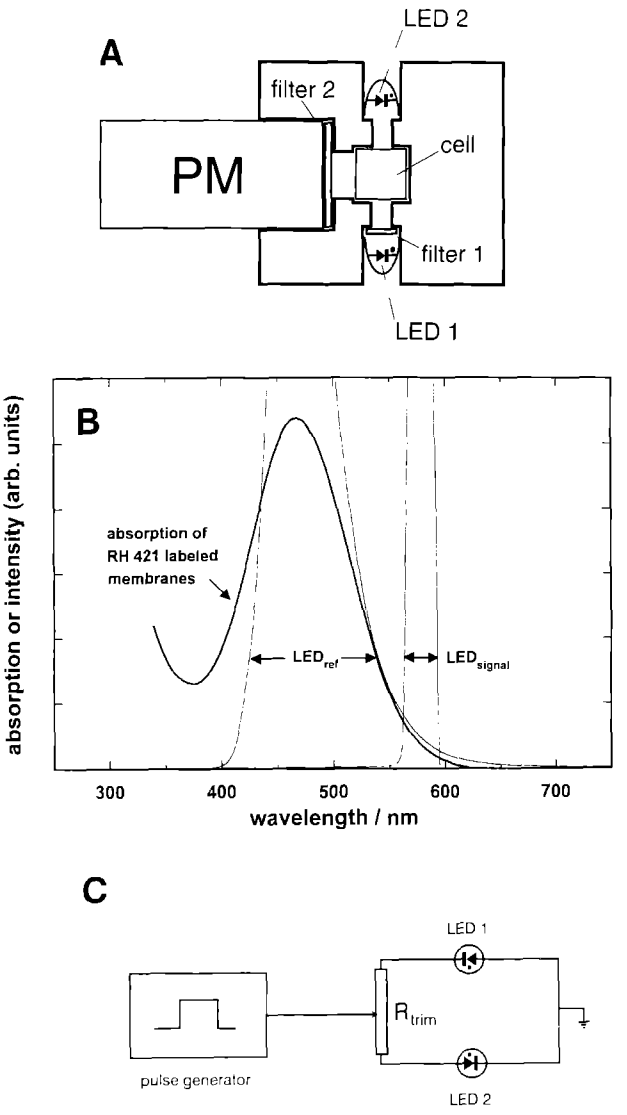

Fig. 1A–C. Principle of the dual wavelength fluorimeter. **A** Cross section through the setup. A standard 12×12 mm^2 glass cuvette is placed in the center of the aluminium block. Two bores, placed opposite to each other, each holds an LED which is mounted in a parabolic reflector. One LED has a narrow-band interference filter in front of the reflector (filter 1). At 90 degrees to the LEDs a photo multiplier (PM) with a filter combination of cut-off filter and narrow-band interference filter (filter 2) in front of the PM entrance window collects the fluorescence emission of the solution in the cell. The whole setup is placed within a PVC housing to shield the apparatus from stray light. The cuvette is accessible by a shutter from above. A Teflon-covered stirring magnet in the cell is underneath the light path of the LEDs and impelled by an electromagnetic device. **B** Absorption spectrum of RH 421-labeled membrane fragments superimposed with the emission spectra of the two LEDs, which emit the electric-field sensitive excitation light, LED$_{signal}$, and the reference light, LED$_{ref}$. **C** Electronic circuit of the instrument, which allows alternate activation of the two LEDs with light pulses of comparable intensities

ter with a maximum at 660 nm and a half width of 30 nm are mounted.

A pulse generator produced a rectangular pulse with voltages between +5 and −5 V to activate alternately the two LEDs, as indicated in Fig. 1C. With a trim resistor, the voltages to the two LEDs were adjusted in such a way that the fluorescence detected in the PM was in the same range of intensity for both wavelengths. The pulse generator was set to a frequency, which still produced rectangular voltage signals at the output of the operational amplifier that transformed the PM current into a voltage signal (gain: 10^6 VA^{-1}).

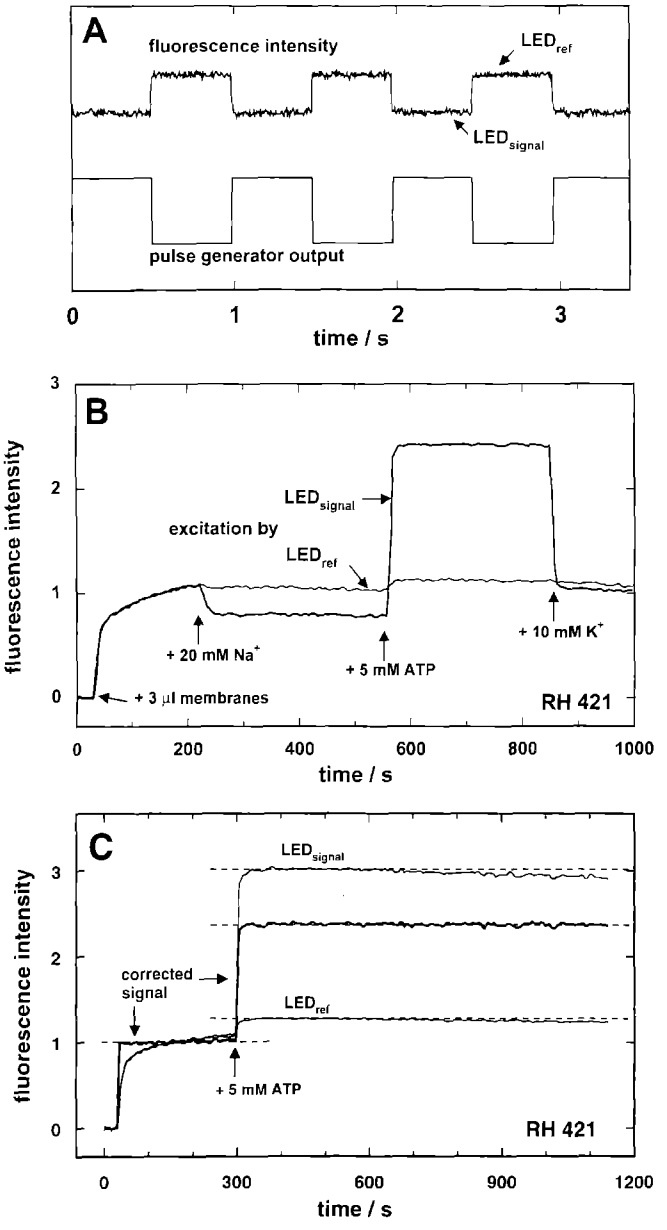

Fig. 2A–C. Signal analysis of the dual-wavelength fluorimeter. **A** Comparison of photomultiplier output and pulse-generator signal. A positive voltage activated the LED$_{signal}$, a negative voltage activated the broad band LED$_{ref}$. The averaged signal of each illumination period is calculated for both LEDs and stored as a data and reference point together with the time, when the voltage changes from positive to negative sign. **B** Representation of an experiment, in which the Na,K-ATPase by successive addition of Na^+, ATP and K^+ is driven through the reaction sequence $E_1 \rightarrow (Na_3)E_1 \rightarrow P\text{-}E_2 \rightarrow E_2(K_2)$. The fluorescence intensity is shown as a function of time for both LEDs, signal (*bold line*) and reference (*thin line*). Upon ATP addition a small visible response in the reference signal can be observed. **C** Effect of the drift correction by calculation of the ratio of the signals, F (LED$_{signal}$)/F (LED$_{ref}$). The dashed lines parallel to the time axis are drawn to guide the eye. They make the point that drift effects are completely canceled out in the corrected signal

The PM output and the voltage signal of the pulse generator were collected in parallel in different channels of a data acquisition board of a PC with sampling frequencies between 100 Hz and 10 kHz, depending on the pulse length of the pulse generator (Fig. 2A). The fluorescence intensities were determined by averaging all data points within each illumination period. The resulting values were collected correspondingly in a data or reference array, according to the sign of pulse signal. In Fig. 2B an experiment is shown in which the Na,K-ATPase molecules are subsequently driven through the reaction sequence $E_1 \rightarrow (Na_3)\ E_1 \rightarrow P\text{-}E_2 \rightarrow E_2(K_2)$ by successive addition of 20 mM Na^+, 5 mM ATP and 10 mM K^+, respectively, to a solution of RH 421-labeled membrane fragments. The lines show the time course of data points, each the average value of one illumination period. The fluorescence excited at λ=585 nm is marked "LED_{signal}" (bold line). The thin line represents the time course of the reference fluorescence, marked LED_{ref}. The ratio of the two signals, $F(LED_{signal})/F(LED_{ref})$, is a drift corrected signal, which is presented or analyzed in all following figures. In Fig. 2C the drift correction effect is demonstrated by an experiment in which 3 µl of membrane-fragment solution was added to a buffer containing 20 mM NaCl, 5 mM $MgCl_2$ and 200 nM RH 421 (at t=30 s). 5 mM ATP was added at t=300 s. Since the dephosphorylation of the enzyme is slow in the absence of K^+, the pumps remained in the (stationary) state $P\text{-}E_2$ for a long period of time owing to the low ATP consumption. The frequency of the pulse generator was set to 1 Hz in this experiment. The corrected signal is shown as bold line in comparison to the fluorescence signals excited by both LEDs. While the fluorescence intensities of both wavelengths increased slowly during the period 30 s < t < 300 s, the corrected signal was stable within 5 s. The fluorescence drift after addition of ATP (t > 300 s) was ~0.3% per minute in the case of each LED signal but disappeared completely after calculation of the quotient (Fig. 2C).

Results

Cytoplasmic binding of sodium ions

Previous publications discussed the fact that the apparent affinity of the binding of Na^+ ions to the sites of the protein facing the cytoplasm depends on the absence or presence of Mg^{2+} ions: typical half binding constants are 0.7 mM in the absence of Mg^{2+} and 7 mM in the presence of 5 mM Mg^{2+} (Glynn 1985; Schwappach et al. 1994). An interdependence of the three bound ions is reflected by the fact that the binding kinetics of Na^+ ions has a Hill coefficient greater than one (Karlish and Stein 1985). In a recent publication a Hill coefficient of 1.8 was determined in the presence of Mg^{2+} by the standard RH 421 method with the rabbit kidney enzyme (Schwappach et al. 1994). This number can be taken as a parameter that indicates cooperative effects in the ion binding. Heyse et al. (1994) suggested that the change of the RH 421 fluorescence intensity is caused mainly by binding of the 'third' Na^+ ion to an uncharged binding site within the protein dielectric.

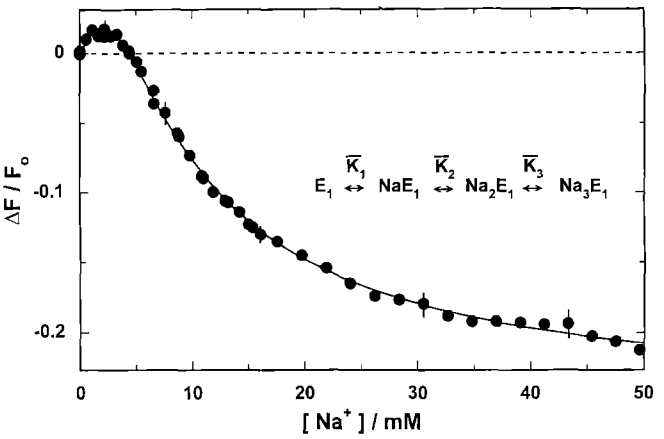

Fig. 3. Na^+ ion binding in the E_1 conformation of the Na,K-ATPase to sites exposed to the cytoplasm, as detected by RH 421 fluorescence changes. Relative fluorescence changes were calculated with respect to the intensity, F_0, in the absence of Na^+. The data points represent the data. Titration series in the concentration range up to 5 mM, 15 mM and 50 mM are superimposed in this figure. The solid line is a fit to the data according to the model presented in the appendix, with the boundary condition $[K^+]=0$ and with the equilibrium dissociation constants, $\overline{K_i}$, (i=1, 2, 3), as is given in Table 1

The Na^+ binding was reinvestigated with the described dual-wavelength fluorimeter. In a fluorescence cell 9 µg Na,K-ATPase were equilibrated in 1 ml buffer containing 25 mM histidine, 0.5 mM EDTA, 10 mM $MgCl_2$ and 200 nM RH 421, pH 7.2. After determination of the initial fluorescence level, F_0, Na^+ ions were added in aliquots from solutions containing 100 mM or 1 M NaCl. For each concentration step the corresponding fluorescence level was determined and the relative change in fluorescence intensity calculated by $\Delta F/F_0=(F[Na]F_0)/F_0$. This experiment was repeated independently over 40 times with several different protein preparations and in concentration ranges between 0 and 5 mM, 15 mM or 50 mM NaCl. The result is presented in Fig. 3. Typical error bars are given for a few data points. The striking difference from previously published findings with a standard single-wavelength setup was a positive fluorescence change between 0 and 4 mM. This behavior contains additional information which was analyzed according to the model discussed in the appendix. The data could be simulated with the function defined in Eq. A10 and equilibrium dissociation constants of $\overline{K_1}=3 \pm 0.2$ mM ($E_1 \leftrightarrow NaE_1$), $\overline{K_2}=5.23 \pm 0.4$ mM ($NaE_1 \leftrightarrow Na_2E_1$), $\overline{K_3}=6 \pm 0.4$ mM ($Na_2E_1 \leftrightarrow Na_3E_1$). This set of numbers was unique in the sense that any change larger than 10% did not allow fits to the data points.

Cytoplasmic binding of potassium ions

Binding of K^+ ions to the E_1 conformation of the Na,K-ATPase did not produce significant changes in the RH 421 fluorescence signal, either in the single-wavelength (Stürmer et al. 1991) or in the dual-wavelength method. To obtain reliable information we made use of the competition between Na^+ and K^+ for the same binding sites, and

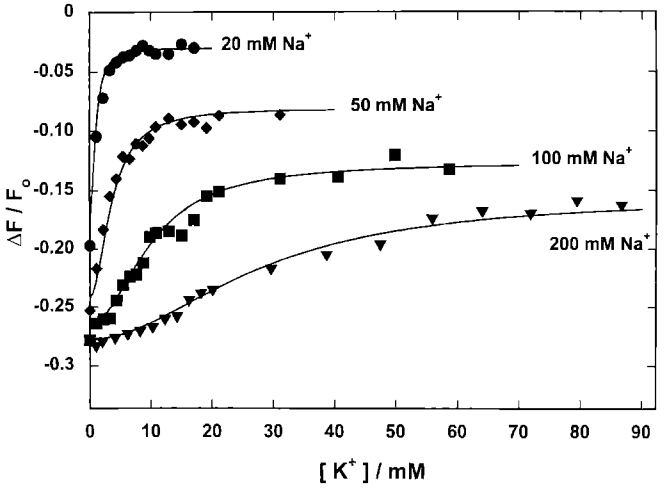

Fig. 4. K^+ ion binding to the sites exposed to the cytoplasmic side of the membrane in the E_1 conformation detected RH 421 fluorescence changes. The membrane fragments were equilibrated in buffers containing the indicated concentrations of NaCl. Aliquots of KCl were added until no further increase of fluorescence could be observed. The lines drawn through the data are fits according to Eq. (A10)

titrated the binding sites with K^+ ions in the presence of different concentrations of Na^+.

In a fluorescence cell 9 µg Na,K-ATPase were equilibrated in 1 ml buffer containing 25 mM histidine, 0.5 mM EDTA, 10 mM $MgCl_2$ and 200 nM RH 421, pH 7.2, at 16 °C. After determination of the initial fluorescence level, F_0, NaCl was added to obtain the indicated concentration of Na^+ (Fig. 4). Subsequently, aliquots of KCl were added until further additions no longer produced significant changes in fluorescence. In Fig. 4, results from experiments are shown, which were performed with four different concentrations of Na^+. To decrease the scatter of the data, two to four identical experiments were averaged and at each concentration of Na^+ three series of experiments were performed with different batches of protein. The plotted curves in Fig. 4 are fits to the data according to Eq. A10 with fixed $\overline{K_i}$ (i = 1, 2, 3), which were determined from the Na^+ titration experiments (Fig. 3). To determine the missing kinetic quantities, $\overline{K_4}$ and $\overline{K_5}$, the K^+ titration curves of all Na^+ concentrations were fitted simultaneously. A single set of values was found which described all experiments: $\overline{K_4} = 0.08 \pm 0.01$ mM and $\overline{K_5} = 0.12 \pm 0.01$ mM. To present an overview, we have plotted the experimentally determined half saturating concentration, $K_{1/2}$, as function of the Na^+ concentration in Fig. 5A. Figure 5B shows the Na^+ concentration dependence of the fluorescence level after addition of Na^+, $\Delta F\ (Na^+)/F_0$ (cf. Fig. 3), and also at saturating K^+ concentrations, $\Delta F_{max}/F_0$. $K_{1/2}$ and $\Delta F\ (Na^+)/F_0$ were fitted by simulation of the experiments (Eq. A10) without further corrections.

The maximum change of the fluorescence, $\Delta F_{max}/F_0$, upon addition of saturating K^+, was overestimated for Na^+ concentrations above 20 mM by the model applied in this paper. In the absence of Na^+ and at high concentrations of K^+, when virtually all pumps can be assumed to be in state $E_2(K_2)$ the fluorescence level was determined to be

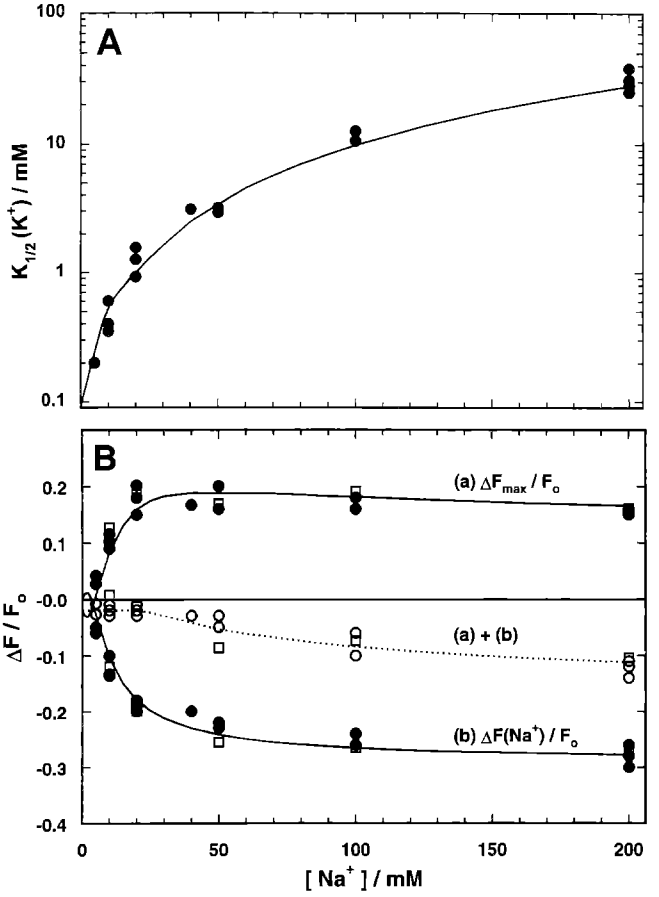

Fig. 5A, B. Analysis of the competition between Na^+ and K^+ ions on the binding sites in conformation E_1 of the Na,K-ATPase. From experiments as shown in Fig. 4 three characteristic numbers have been taken: **A** the half-saturating concentration, $K_{1/2}$, of K^+ binding, **B** the fluorescence level in the presence of the indicated Na^+ concentration and in the absence of K^+, $\Delta F(Na^+)/F_0$, and in the presence of saturating K^+, $\Delta F_{max}/F_0$. The dependence of these experimental quantities on Na^+ concentration (*data points*) is compared with the discussed equilibrium binding model in the appendix (*lines*). Circles represent experiments in low ionic strength, squares represent experiments in buffer with an ionic strength of 200 mM (maintained by choline chloride)

$f_6 = -0.03$. In the presence of Na^+ ions in the buffer and sufficiently high concentrations of K^+ ions all proteins should again be in states K_2E_1 or E_2 (K_2) with a specific fluorescence level of –0.03. In Fig. 5B the open symbols represent the corresponding saturating fluorescence levels from the experiments. To describe $\Delta F_{max}/F_0$ correctly, a phenomenological correction factor was introduced. The origin of this fluorescence reduction is not understood so far. Control experiments exclude an artifact of ionic strength.

Discussion

The Post-Albers scheme represents a consecutive (or "ping-pong") mechanism, in which Na^+ and K^+ ions are transported in different parts of the pump cycle. This property of the transport mechanism was demonstrated by dif-

ferent flux modes of the protein (for review see Glynn 1985). Implicit in this scheme is the fact that the ion binding sites have to release one species of ion before binding another one when the sites are exposed to the aqueous phase. In principle, it is not necessary for the binding affinities to change when the conformation of the protein changes, although such a feature produces a kinetic advantage (Läuger 1991). Experiments performed to determine apparent affinities have revealed that, in the case of the Na,K-ATPase, there is high affinity Na^+ binding in the E_1 conformation and high affinity K^+ binding in the E_2 conformation (for review, see Stein 1986).

Previous studies of ion-binding affinities were performed mainly in an indirect manner, since only alterations of the pump protein consequent to ion binding or release could be detected. Approaches have included analyzing the complete transport cycle, by uptake or efflux of tracer ions in red blood cells or vesicles (Garray and Garrahan 1977; Sachs 1977; Blostein 1983; Karlish and Stein 1985), by potential-sensitive dyes (Apell and Marcus 1986), or by measuring enzymatic activity (Cornelius and Skou 1988; Cornelius 1992). In experiments in which the pump did not run through the whole cycle, ion occlusion was measured (Glynn and Richards 1982; Glynn 1984; Shani et al. 1987), the intrinsic fluorescence (Karlish and Yates 1987) or conformation-sensitive fluorescence labels, fluorescein 5′-isothiocyanate (Karlish 1980; Rephaeli et al. 1986) or eosin (Esmann 1994) were used. Smirnova and Faller (1993) applied fluorescein 5′-isothiocyanate in stopped-flow experiments and found kinetic evidence for two potassium dissociation constants, which differed by a factor of 4. To describe the time dependence and amplitude of the relaxation processes with a two site model, they used ratios of $\overline{K_4}/\overline{K_5}$ in the range between 3.7 ± 1.8 and 5.0 ± 2.1. From these findings they concluded the existence of two independent and identical sites. The fact that their absolute values of $\overline{K_4}$ and $\overline{K_5}$ were 2.8 ± 0.9 mM and 14.0 ± 1.4 mM, respectively, indicates that an additional, kinetic process contributed, which is insignificant in equilibrium titrations as in our experiments, in which the values of $\overline{K_4}$ and $\overline{K_5}$ were both in the range of 0.1 mM.

We did not introduce a separate reaction step for the transition $K_2E_1 \leftrightarrow E_2(K_2)$, since it is a substrate independent (monomolecular) reaction, which is strongly shifted to the right by a ratio of 1/1000 in the absence of ATP (Heyse et al. 1994). If the state K_2E_1 is implemented, the value of $\overline{K_4}$ remains unchanged. The constant $\overline{K_5}$ in the discussed model has to be replaced by $\overline{K'_5} \cdot \overline{K'_6}$, where the reaction $KE_1 \leftrightarrow K_2E_1$ is controlled by $\overline{K'_5}$, and $K_2E_1 \leftrightarrow E_2(K_2)$ by $\overline{K'_6}$. If $\overline{K'_6}$=1/1000, the equilibrium constant $\overline{K'_5}$ is calculated to be 80 mM. This result, $\overline{K'_5} \gg \overline{K'_4}$, is in agreement with the explanation given for the hyperbolic activation of the K^+-K^+ exchange by cytoplasmic K^+ (Karlish and Stein 1985).

Direct access to single ion binding steps is possible only when observable quantities can be found that allow discrimination between states with different numbers of ions bound. The dual-wavelength detection of RH 421 fluorescence intensities provides such a possibility. Although there is a general agreement that dyes of this class respond to changes of the (local) electric field in their environment, the mechanism is not yet understood completely (Grinwald et al. 1982; Ephardt and Fromherz 1989; Bühler et al. 1991; Clarke et al. 1992). However, an influence of conformational changes of the Na,K-ATPase on the RH 421 signal was excluded by control experiments with the membrane preparations used in the present work (Stürmer et al. 1991; Heyse et al. 1994).

A direct determination of a specific fluorescence level, f[X], was possible for three out of the six states in the sequence $(Na_3)E_1, \ldots, E_2(K_2)$ (Eq. (1)). In the absence of Na^+ and K^+ ions, the fluorescence level $f[E_1]$ was defined as the reference and set to be 0. Saturating concentrations of Na^+ in the absence of K^+ ions maintained the enzyme quantitatively in state Na_3E_1, with $f[Na_3E_1] = -0.26 \pm 0.02$. The fluorescence level $f[E_2(K_2)] = -0.03 \pm 0.002$ was obtained by forcing the pump into state $E_2(K_2)$ by saturating K^+ concentrations and in the absence of Na^+. The remaining two levels in the Na^+-binding branch were obtained by fitting the Na^+ titration curves (Fig. 3). Since they have positive levels, $f[NaE_1] = 0.018 \pm 0.001$ and $f[Na_2E_1] = 0.11 \pm 0.003$, in contrast to $f[Na_3E_1]$, it was possible to determine them unequivocally. The final missing level, $f[KE_1] = -0.015 \pm 0.01$, could be varied by a factor of ~2, since it contributed only marginally to fluorescence intensity (<1% of the total signal).

The surprising result that the fluorescence levels of states NaE_1 and Na_2E_1 have to be set positive to explain the Na^+ concentration dependence (Fig. 3) does not have its origin in an electrogenic effect. Control experiments with a single wavelength fluorescence spectrophotometer revealed a monotonic shift of the absorption spectrum of RH 421 towards shorter wavelengths when the Na^+ concentration was increased (not shown), as expected (Bühler et al. 1991). The finding that the ratio $F(LED_{signal})/F(LED_{ref})$ was biphasic as function of the Na^+ concentration was a consequence of the incomplete overlap of the LED_{ref} emission spectrum and the RH 421 absorption spectrum (Fig. 1B). For very small (blue) shifts of the absorption spectrum of RH 421 as induced by the binding of the first two Na^+ ions, the LED_{ref} excited fluorescence dropped faster than that of the LED_{signal}.

The phenomenological correction factor, which was introduced to account for the reduction of the fluorescence, $\Delta F_{max}/F_0$, in high Na^+ concentrations, is different from 1 at Na^+ concentrations above 20 mM (Fig. 5B). This observation could be caused by a Na^+-specific or by a general ionic strength effect. To rule out the latter, we repeated the experiments in the presence of 200 mM choline chloride and found no significant influence on the fluorescecence changes (squares in Fig. 5B). Shani et al. (1987) found an influence of Na^+ concentrations above 30 mM on Rb^+ occlusion, which they described as a 'non-competitive antagonistic effect'. This observation could be caused by the same mechanism, whose origin has to be revealed by further investigations.

The equilibrium dissociation constants for all five steps of Eq. (1) are shown in Table 1. They were obtained by fitting simultaneously all data presented. The variations of the values in Table 1 represent a confidence interval, in which all experiments (Figs. 3–5) could be fitted with an acceptable performance. No alternative set of constants

Table 1. The experimentally determined set of equilibrium dissociation constants (± standard deviation) for cytoplasmic binding of Na^+ and K^+ ions. The buffer contained 25 mM histidine, 0.5 mM EDTA, 10 mM $MgCl_2$, pH 7.2, besides various concentrations of Na^+ and K^+. The temperature was 16 °C. All data presented could be simulated with these kinetic constants and no additional adjustments were necessary

Reaction step	Constant	Value/mM
$Na_3E_1 \leftrightarrow Na_2E_1$	$\overline{K_3}$	6.5 ± 0.4
$Na_2E_1 \leftrightarrow NaE_1$	$\overline{K_2}$	5.2 ± 0.4
$NaE_1 \leftrightarrow E_1$	$\overline{K_1}$	3.0 ± 0.2
$E_1 \leftrightarrow KE_1$	$\overline{K_4}$	0.08 ± 0.01
$KE_1 \leftrightarrow E_2(K_2)$	$\overline{K_5}$	0.12 ± 0.01

could be found. The observation that $\overline{K_1}$ and $\overline{K_2}$ differed by less than a factor of 2 may be discussed in the light of the fact that random binding or release of ions from two identical and independent binding sites would produce, owing to statistical reasons, a difference of a factor of 4 between $\overline{K_1}$ and $\overline{K_2}$. The same argument is valid for the K^+-binding steps, $\overline{K_4}$ and $\overline{K_5}$, which are different also by less than a factor of 2. For Rb^+ ions (as congener of K^+) ordered binding and release was found (Forbush 1987), which excludes the idea of independent binding sites. Assuming the same kind of cooperativity for Na^+ ions would not be in conflict with the results of previous investigations on cytoplasmic Na^+ binding.

Studies of the sodium-rubidium antagonism in the E_1 form the Na,K-ATPase by analysis of the kinetics of concentration-jump experiments led to results which were analyzed by a model that implemented states with 'mixed' populations, such as E_1Rb_2Na or E_1RbNa_2, to account for the complex behavior found in these experiments (Esmann 1994). All 'steady state' experiments presented in this paper could be fitted satisfactorily by the linear reaction chain of Eq. (1) without 'mixed' populations of the sites. Owing to the small differences of the specific fluorescence of states with one or two ions bound and owing to the low proposed probability of the 'mixed' populations on the other hand, the existence of those states cannot be excluded.

The small size of the specific fluorescence changes that are produced by binding of (the first) two Na^+ or K^+ ions are in agreement with the proposal that these binding sites have two negative charges at the dielectric protein/water interface (Stürmer et al. 1991; Heyse et al. 1994). Binding of the third Na^+ ion is assumed to occur to a neutral site inside the protein with a dielectric depth of 0.25 (Heyse et al. 1994). Taking into account this number as well as the model discussed in the Appendix and the constants of Table 1, predictions can be made on the influence of the membrane potential on a shift of the apparent half-saturating ion concentration for the Na^+ binding, $K_{1/2}$. When a trans-membrane potential of 25 mV is applied, a shift of $K_{1/2}$ in the order of 10% is predicted.

The affinity of the ion binding sites in state E_1 is generally assumed to be higher for Na^+ ions (Simons 1974). The results of Figs. 4 and 5 on the other hand show that the equilibrium dissociation constants for K^+ ions are significantly lower than for Na^+. Indeed the affinity of the 'empty' pump in state E_1 for K^+ is 38 times higher than for Na^+. The high K^+ affinity is in agreement with previous studies (Karlish 1980; Shani et al. 1987), which found half saturating concentrations, $K_{1/2}$, in state E_1 for K^+/Rb^+ ions in the range of 0.1–0.2 mM. Esmann (1994) reported a $K_{1/2}$ of 0.016 mM for Rb^+ occlusion. Assuming physiological ion concentrations (150 mM K^+ and 5 mM Na^+) the model presented in the appendix predicts an almost complete population of state $E_2(K_2)$ in the absence of ATP. This result seems to be in opposition to the requirements of a living cell. However, these experiments were performed in the absence of ATP to confine the pump to the states of Eq. (1) (Glynn and Richards 1982; Forbush 1987). The influence of ATP was investigated by Shani et al. (1987), who found that ATP shifts $K_{1/2}$ of K^+ binding by almost a factor of 10 to higher concentrations. On the other hand the phosphorylation of the enzyme by ATP in state Na_3E_1 drains this state continuously and thus produces under turnover conditions an apparent Na^+ affinity in the range of 10–20 mM (Sachs 1977; Karlish and Stein 1985; Apell and Marcus 1986). This is also in agreement with early measurements of Skou (1957), who showed that high K^+ and low Na^+ (cytoplasmic) concentrations have a rate-limiting effect on the turnover of the Na,K-ATPase.

The conclusions to be drawn from these results are that the intrinsic ion binding affinity is higher for K^+ than for Na^+ ions in both principal conformations, E_1 and E_2. The binding affinities of the extracellularly presented sites for K^+ ions are in the range 0.1–0.3 mM (Stein 1986; Forbush 1987; Bühler and Apell 1994) and indicate that they are hardly changed by the E_1-E_2 conformation transition. A difference in binding affinities could be observed for Na^+ binding, which is higher in conformation E_1, 3–7 mM (Table 1), than in E_2, where apparent affinities of 50–2500 mM have been found (Heyse et al. 1994). The 'high' apparent affinity for Na^+ ions, which promotes the Na,K-ATPase through its pump cycle to perform its physiological function in the presence of K^+ ions, is a consequence of the kinetics of the two partial reactions, $E_2(K_2) \leftrightarrow ATP \cdot E_2(K_2)$ and $Na_3E_1 \cdot ATP \leftrightarrow (Na_3)E_1$-P, both of which are strongly shifted in the forward direction (to the right) in the presence of ATP (Karlish et al. 1982). These two reactions precede and follow the ion release and binding steps, $K_2E_1 \cdot ATP \leftrightarrow \ldots \leftrightarrow Na_3E_1 \cdot ATP$, and thus give rise to the functional Na,K exchange despite the unfavorable intrinsic binding affinities of the E_1 conformation.

Acknowledgements. We thank M. Roudna and G. Witz for excellent technical assistance and Drs. D. C. Gadsby and S. J. D. Karlish for stimulating discussions. This work was financially supported by the Deutsche Forschungsgemeinschaft (Sonderforschungsbereich 156).

Appendix

In the generally accepted Post-Albers cycle of the Na,K-ATPase one set of binding sites binds alternately Na^+ and K^+ ions ("ping-pong mechanism"). In the absence of ATP and inorganic phosphate, P_i, the enzyme is confined to the

states

$$Na_3E_1 \xleftrightarrow{K_3} Na_2E_1 \xleftrightarrow{K_2} NaE_1 \xleftrightarrow{K_1} E_1 \xleftrightarrow{K_4} KE_1 \xleftrightarrow{K_5} E_2(K_2),$$

where the values of K_i depend on the concentrations of Na^+ (i=1, 2, 3) or K^+ (i=4, 5). Analyzing this reaction scheme under steady state conditions, each reaction step can be described by a linear equation as a function of the fractional occupancy of the participating two states, the ion concentration and the corresponding equilibrium dissociation constant, $\overline{K_i}$. For example

$$[NaE_1] = \frac{[Na^+]}{\overline{K}_1} \cdot [E_1] \tag{A1}$$

Taking into account the boundary condition

$$[Na_3E_1] + [Na_2E_1] + [NaE_1] + [E_1] + [KE_1] + [E_2(K_2)] = 1 \tag{A2}$$

The population of all 6 states can be calculated as function of the ion concentrations and the corresponding equilibrium dissociation constants. With the definition

$$D = \overline{K_1}\,\overline{K_2}\,\overline{K_3} \cdot (\overline{K_5} \cdot [K^+] + [K^+]^2) + \overline{K_4}\,\overline{K_5} \cdot (\overline{K_1}\,\overline{K_2}\,\overline{K_3} + \overline{K_2}\,\overline{K_3} \cdot [Na^+] + \overline{K_3} \cdot [Na^+]^2 + [Na^+]^3) \tag{A3}$$

the solutions of the system of equations are

$$[Na_3E_1] = \frac{\overline{K}_4\,\overline{K}_5 \cdot [Na^+]^3}{D} \tag{A4}$$

$$[Na_2E_1] = \frac{\overline{K}_3\,\overline{K}_4\,\overline{K}_5 \cdot [Na^+]^2}{D} \tag{A5}$$

$$[NaE_1] = \frac{\overline{K}_2\,\overline{K}_3\,\overline{K}_4\,\overline{K}_5 \cdot [Na^+]}{D} \tag{A6}$$

$$[E_1] = \frac{\overline{K}_1\,\overline{K}_2\,\overline{K}_3\,\overline{K}_4\,\overline{K}_5}{D} \tag{A7}$$

$$[KE_1] = \frac{\overline{K}_1\,\overline{K}_2\,\overline{K}_3\,\overline{K}_5 \cdot [K^+]}{D} \tag{A8}$$

$$[E_2(K_2)] = \frac{\overline{K}_1\,\overline{K}_2\,\overline{K}_3 \cdot [K^+]^2}{D}. \tag{A9}$$

To calculate the fluorescence signals, the specific fluorescence levels of the different states, f [x], have to be defined. For three states, the corresponding values can be determined experimentally by appropriate selection of the ionic composition of the buffer. These values showed variations in the range of 15%, dependent on the concentration of active protein in the membrane preparation. Average values over 14 different preparations were:

$f[E_1] \equiv f_1 = 0,$	0 Na^+ and 0 K^+ in buffer,
$f[Na_3E_1] \equiv f_4 = -0.26$	saturating Na^+, 0 K^+ in buffer,
$f[E_1(K_2)] \equiv f_6 = -0.03,$	0 Na^+, saturating K^+ in buffer.

The remaining levels have been obtained by fitting all experimental data simultaneously with the same set of values:

$$f[NaE_1] \equiv f_2 = 0.018,$$
$$f[Na_2E_1] \equiv f_3 = 0.11$$
$$f[KE_1] \equiv f_5 = -0.015.$$

On the basis of these definitions, the experiments presented in this paper can be simulated with the following function:

$$\frac{\Delta F}{F_0} = f_1 \cdot [E_1] + f_2 \cdot [NaE_1] + f_3 \cdot [Na_2E_1] + f_4 \cdot [Na_3E_1] + f_5 \cdot [KE_1] + f_6 \cdot [E_2(K_2)]. \tag{A10}$$

References

Apell H-J, Marcus MM (1986) ($Na^+ + K^+$)-ATPase in artificial lipid vesicles: influence of the concentration of mono- and divalent cations on the pumping rate. Biochim Biophys Acta 862: 254–264

Argüello JM, Kaplan JH (1994) Glutamate 779, an intramembrane carboxyl, is essential for monovalent cation binding by the Na,K-ATPase. J Biol Chem 269: 6892–6899

Blostein R (1983) The influence of cytoplasmic sodium concentration on the stoichiometry of the sodium pump. J Biol Chem 258: 12228–12232

Bühler R, Apell H-J (1994) Sequential potassium binding in the E_2-P conformation of the Na,K-pump. Biophys J A236 (Abstract)

Bühler R, Stürmer W, Apell H-J, Läuger P (1991) Charge translocation by the Na,K-pump: I. Kinetics of local field changes studied by time-resolved fluorescence measurements. J Membrane Biol 121: 141–161

Capasso JM, Hoving S, Tal DM, Goldshleger R, Karlish SJD (1992) Extensive digestion of Na^+, K^+-ATPase by specific and non-specific proteases with preservation of cation occlusion sites. J Biol Chem 267: 1150–1158

Clarke RJ, Schrimpf P, Schöneich M (1992) Spectroscopic investigations of the potential-sensitive membrane probe RH 421. Biochim Biophys Acta 1112: 142–152

Cornelius F (1992) Cis-allosteric effects of cytoplasmic Na^+/K^+ discrimination at varying pH. Low-affinity multisite inhibition of cytoplasmic K^+ in reconstituted Na^+/K^+-ATPase engaged in uncoupled Na^+-efflux. Biochim Biophys Acta 1108: 190–200

Cornelius F, Skou JC (1988) Non-equivalent cytoplasmic Na^+ sites and their susceptibility to transmembrane interaction from extracellular Na^+. In: The Na^+,K^+-Pump, Part A: Molecular aspects. Alan R Liss, New York, pp 485–492

Ephardt H, Fromherz P (1989) Fluorescence and photo isomerization of an amphiphilic amino-stilbazolium dye as controlled by the sensitivity of radiationless desactivation to polarity and viscosity. J Phys Chem 93: 7717–7725

Esmann M (1994) Influence Na^+ on Conformational States in Membrane-Bound Renal Na,K-ATPase. Biochemistry 33: 8558–8565

Forbush III B (1987) Rapid release of ^{42}K or ^{86}Rb from two distinct transport sites on the Na,K-pump in the presence of P_i or vanadate. J Biol Chem 262: 11116–11127

Forbush III B, Klodos I (1991) Rate limiting steps in Na translocation by the Na/K pump. In: The Sodium Pump. Structure, Mechanism and Regulation. Kaplan JH, De Weer P (eds) Rockefeller University Press, New York, pp 211–225

Gadsby DC, Rakowski RF, De Weer P (1993) Extracellular access to the Na,K pump: pathway similar to ion channel. Science 260: 100–103

Garay RP, Garrahan PJ (1973) The interaction of sodium and potassium with the sodium pump in red cells. J Physiol 231: 297–325

Glynn IM (1985) The Na^+,K^+-transporting adenosine triphosphatase. In: The Enzymes of Biological Membranes. Martonosi AN (ed) 2nd edn. Vol. 3. New York, Plenum Press, pp 35–114

Glynn IM, Richards DE (1982) Occlusion of rubidium ions by the sodium-potassium pump: its implications for the mechanism of potassium transport. J Physiol 330: 17–43

Glynn IM, Hara Y, Richards DE (1984) The occlusion of sodium ions within the mammalian sodium-potassium pump: its role in sodium transport. J Physiol 351: 531–547

Goldshleger R, Tal DM, Moorman J, Stein WD, Karlish SJD (1992) Chemical modifications of Glu953 of the α chain of Na^+,K^+-ATPase associated with inactivation of cation occlusion. Proc Natl Acad Sci, USA 89:6911–6915

Grinvald A, Hildesheimer R, Farber IC, Anglister L (1982) Improved fluorescent probes for the measurement of rapid changes in membrane potential. Biophys J 39:301–308

Heyse S, Wuddel I, Apell H-J, Stürmer W (1994) Partial reactions of the Na,K-ATPase: Determination of rate constants. J Gen Physiol 104:197–240

Homerada H, Nozaki T, Matsui H (1987) Interaction of sodium and potassium ions with Na,K-ATPase. III. Cooperative effect of ATP and Na^+ on complete release of K^+ from E_2K. J Biochem 101:789–793

Jensen J, Nørby JG, Ottolenghi P (1984) Binding of sodium and potassium to the sodium pump of pig kidney evaluated from nucleotide-binding behaviour. J Physiol 346:219–241

Jørgensen PL (1974) Isolation of the (Na^+ + K^+)-ATPase. Methods Enzymol 32:277–290

Jørgensen PL (1992) Na,K-ATPase, structure and transport mechanism. In: Molecular aspects of transport proteins. DePont JJHHM (ed) Elsevier, Amsterdam, pp 1–26

Jørgensen PL, Andersen JP (1988) Structural basis for E_1-E_1 conformational transitions in Na,K-pump and Ca-pump proteins. J Membrane Biol 103:95–120

Karlish SJD (1980) Characterization of conformational changes in (Na,K) ATPase labeled with fluorescein at the active site. J Bioenerg Biomembr 12:111–136

Karlish SJD, Pick U (1981) Sidedness of the effects of sodium and potassium ions on the conformational state of the sodium-potassium pump. J Physiol 312:505–529

Karlish SJD, Stein WD (1985) Cation activation of the pig kidney sodium pump: transmembrane allosteric effects of sodium. J Physiol 359:119–149

Karlish SJD, Yates DW (1978) Tryptophan fluorescence of (Na^+ + K^+)-ATPase as a tool for study of the enzyme mechanism. Biochim Biophys Acta 527:115–130

Karlish SJD, Lieb WR, Stein WD (1982) Combined effects of ATP and phosphate on rubidium exchange mediated by Na-K-ATPase reconstituted into phospholipid vesicles. J Physiol 328:333–350

Karlish SJD, Goldshleger R, Stein WD (1990) Identification of a 19 kDa C-terminal tryptic fragment of the alpha chain of Na^+,K^+-ATPase, Essential for occlusion and transport. Proc Natl Acad Sci, USA 87:4566–4570

Klodos I, Forbush III B (1988) Rapid conformational changes of the Na/K pump revealed by a fluorescent dye, RH 160. J Gen Physiol 92:46a

Läuger P (1991) Electrogenic Ion Pumps. Sinauer Associates, Sunderland, MA, pp 1–313

Lowry OH, Rosebrough NJ, Farr AL, Randall RJ (1951) Protein measurement with the folin phenol reagents. J Biol Chem 193:265–275

Pratap PR, Robinson JD, Steinberg MI (1991) The reaction sequence of the Na^+/K^+-ATPase: rapid kinetic measurements distinguish between alternative schemes. Biochim Biophys Acta 1069:288–298

Rephaeli A, Richards D, Karlish SJD (1986) Conformational transitions in fluorescein-labeled (Na,K)-ATPase reconstituted into phospholipid vesicles. J Biol Chem 261:6248–6254

Sachs JR (1977) Kinetic evaluation of the Na-K pump reaction mechanism. J Physiol 273:489–514

Sagar A, Rakowski RF (1994) Access channel model for the voltage dependence of the forward-running Na^+/K^+ pump. J Gen Physiol 103:869–894

Shani M, Goldshleger R, Karlish SJD (1987) Rb^+ occlusion in renal (Na^+ + K^+)-ATPase characterized with a simple manual assay. Biochim Biophys Acta 904:13–21

Schwappach B, Stürmer W, Apell H-J, Karlish SJD (1994) Binding of Sodium Ions and Cardiotonic Steroids to Native and Selectively Trypsinized Na,K Pump, Detected by Charge Movement. J Biol Chem 269:21620–21626

Schwartz A, Nagano K, Nakao M, Lindenmayer GE, Allen JC (1971) The sodium- and potassium-activated adenosinetriphosphatase system. Methods Pharmacol 1:361–388

Simons TJB (1974) Potassium : potassium exchange catalysed by the sodium pump in human red cells. J Physiol 237:123–155

Skou JC (1975) The (Na^+ + K^+)-activated enzyme system and its relationship to transport of sodium and potassium. Q Rev Biophys 7:401–434

Skou JC, Esmann M (1980) Effects of ATP and protons on the Na^+:K^+ selectively of the (Na^+ + K^+)-ATPase studied by ligand effects on intrinsic and extrinsic fluorescence. Biochim Biophys Acta 601:386–402

Smirnova IN, Faller LD (1993) Mechanism of K^+ Interaction with Fluorescein 5′-Isothiocyanate-modified Na^+,K^+-ATPase. J Biol Chem 268:16120–16123

Stein WD (1986) Transport and diffusion across cell membranes. Chapter 6, Primary active transport systems: chemiosmosis. Academic Press, Orlando, pp 475–512

Stürmer W, Apell H-J (1992) Fluorescence study on cardiac glycoside binding to the Na,K-pump: Ouabain binding is associated with movement of electric charge. FEBS Lett 300:1–4

Stürmer W, Bühler R, Apell H-J, Läuger P (1991) Charge translocation by the Na,K-pump: Ion binding and release studied by time-resolved fluorescence measurements. In: The Sodium Pump. Recent Developments. Kaplan JH, De Weer P (eds) Rockefeller University Press, New York, pp 531–536

Wuddel I, Stürmer W, Apell H-J (1994) Dielectric coefficients of the extracellular release of sodium ions. In: The Sodium Pump. Bamberg E, Schoner W (eds) Steinkopff, Darmstadt, pp 577–580